

## Relationship between carrier density and corrosion behavior of acrylic polyurethane coated galvanized steel system in 3.5% NaCl solution

L. Lu\*, T. L. Lu, M. Z. Ding, J. Gao

Corrosion and Protection Center, University of Science and Technology Beijing, Beijing100083, China

\*E-mail: [lulin315@126.com](mailto:lulin315@126.com)

Received: 7 May 2019 / Accepted: 14 July 2019 / Published: 5 August 2019

---

Carrier density (CD) was adopted to investigate the corrosion process of acrylic polyurethane-coated galvanized steel in 3.5% NaCl solution by using the Mott–Schottky (M-S) analysis technique. The impedance at 0.01 Hz was used to evaluate the corrosion performance of the coating system as well. Corrosion products formed during the degradation process were detected by X-ray diffraction (XRD) and scanning electron microscopy (SEM). Results showed that the CD of the coating system was approximately  $10^{14} \text{ cm}^{-3}$ , which was the same as the order of a semiconductor, during the early immersion stage. Subsequently, the CD of the coating system increased with the decrease in  $|Z|_{0.01\text{Hz}}$ . However, the CD decreased and the low-frequency impedance increased at day 4. This condition differed from the overall tendency and indicated that the corrosion process of the coating system was hindered. The reason could be attributed to the blocking effect of corrosion products  $\text{Zn}_5(\text{CO}_3)_2(\text{OH})_6$  and  $\text{Zn}_5(\text{OH})_8\text{Cl}_2 \cdot \text{H}_2\text{O}$ , which were generated at the interface of galvanized steel.

---

**Keywords:** electrochemical procedure; carrier density; organic coating; semiconductor; coating degradation

### 1. INTRODUCTION

In recent decades, many kinds of techniques, such as EIS, LEIS, and SKP, have been applied to organic coating systems for investigating the involved electrochemical procedure [1-5]. Consequently, several parameters ( $R_c$ ,  $C_d$ ,  $|Z|_{0.01\text{Hz}}$ , and  $V_K$ ) are used to characterize the corrosion progress of the coating system [6]. Among them, the conductivity of coating system has been used to characterize the shielding property of the coating system, because it manifests the migration of chargers or ions during electrochemical processes. Hamada measured the resistivity of degraded organic films by using DC method; and found that the increase in conductivity was attributed to the trapped ions in the coating

during soaking process [7]. In fact, the conductivity of the whole coating system was not only determined by coating resistance, but also involved in the electrochemical reactions occurred at the interface between the coating and the substrate. That is to say, the charge carriers include not only the charged ions but the electrons, generating from the anodic dissolution of metal substrate. In most literatures, these procedures were characterized with the resistances at different interfaces respectively, such as the coating resistance and the charge transfer resistance, which were extracted by the equivalent circuit fitting of EIS data [8,9]. However, the fitting results are highly dependent on the choice of the circuits, which sometimes are ambiguous and misleading [10-12]. In addition,  $|Z|_{0.01\text{Hz}}$  was used to present the shielding effect of coatings, which was hard to reflect the charge transfer process occurred at the double capacitance layer [13]. Therefore, it is necessary to put forward a uniform parameter to depict the migration process of charges involved in all stages of coating failure. Zhong [14-17] applied the potential-capacitance measurement method in the anti-rust oil film/stainless steel electrode system to observe the conductive behavior during the degradation of the film. It was proposed that the anti-rust oil film had a transition from insulator to semiconductor during the degradation process, which was due to the formation of space charge layer resulting from ion corroding. The same method was also applied in the carbon steel/epoxy resin system. It was found that, at the initial stage of immersion, the conductive behavior of the organic coating was similar to that of semiconductors, and the metal/epoxy formed a Metal-Insulator-Semiconductor structure (MIS). However, the above researches were only involved in the initial stage of degradation, and it was seldom to investigate the applicability of the method to characterize the interface reactions during the final stages of coating failure, especially after corrosion products were formed at the interface.

In light of this, carrier density (CD), a parameter presenting the conductive behavior of semiconductor has been introduced to this paper to monitor all degradation procedures of the coating system in NaCl solution with the aid of Mott-Schottky (M-S) analysis technique. As a complementary,  $|Z|_{0.01\text{Hz}}$  was also adopted to describe the corrosion process of the system at the same time. Based on these, the applicability of CD to coating system and the relationship between the changing tendency of CD and corrosion progress are clarified.

## 2. EXPERIMENTAL

### 2.1 Preparation of sample

Samples were composed of a sheet of hot-dip galvanized steel sheet (Bao Steel, China) and a layer of acrylic polyurethane varnish coating. The paint was prepared with resin, curing agent and diluents with a weight ratio of 4:1:1. The paint used in this experiment was supplied by the commercial producer (Beijing hongshi paint Co. Ltd, China). The substrate was degreased with acetone and the coating was applied using a drawn down bar with a thickness of  $25 \pm 5 \mu\text{m}$ . In order to exclude experimental error, three parallel samples were prepared and tested for each measurement.

## 2.2 Experimental methods

### 2.2.1 Electrochemical impedance spectroscopy

EIS measurements were conducted with PARSTAT 2273 (Princeton, USA) instrument in 3.5% NaCl solution. Platinum plate was served as the counter electrode, a saturated calomel electrode as the reference electrode, and coated galvanized sheet as the working electrode with the working area of 1 cm<sup>2</sup>. The applied frequency was ranged from 100kHz to 10mHz, with the amplitude of the voltage single of 10mV.

### 2.2.2 M-S analysis technique

Along with EIS measurement, C-U curves were measured with the applied potential from -0.9V to -0.1V vs. SCE. The test frequency was 1k Hz. Theoretically, the capacitance-potential relationship can be expressed as M-S Equation [18].

For an N-type semiconductor, the relationship can be expressed in equation 1.

$$\frac{1}{C_{sc}^2} = \frac{2}{\epsilon\epsilon_0 e N_D} \left( U - U_{fb} - \frac{kT}{e} \right) \quad (1)$$

For a P-type semiconductor, the expression can be shown as equation 2.

$$\frac{1}{C_{sc}^2} = -\frac{2}{\epsilon\epsilon_0 e N_A} \left( U - U_{fb} - \frac{kT}{e} \right) \quad (2)$$

Where  $C_{sc}$  is the capacitance of the space charge layer,  $\epsilon$  is the dielectric constant of the semiconductor,  $\epsilon_0$  is the vacuum permittivity ( $8.854 \times 10^{-14}$  F/cm),  $e$  is the electron charge,  $N_D$  and  $N_A$  are the donor and acceptor densities (cm<sup>-3</sup>),  $k$  is the Boltzmann constant ( $1.38 \times 10^{-23}$  J/K),  $T$  is the absolute temperature,  $U$  is the applied potential and  $U_{fb}$  is the flat band potential.

In Mott-Schottky analysis, assuming that the capacitance of the double layer can be neglected, the measured capacitance  $C$  is equal to the space charge  $C_{sc}$  [19,20]. Therefore,  $N_A$  and  $N_D$  can be obtained according to the slope, and flat band  $U_{fb}$  can be obtained according to the interception. With the decrease of the slope, the carrier density increases.

### 2.2.3 X-ray diffraction

An X-ray diffractometer (Smartlab, USA) was carried out to detect the composition of corrosion products at the coating/metal interface. The diffractometer was operated at a voltage of 40 kV and current of 30 mA using CuK $\alpha$  radiation.

### 2.2.4 Microscopy

Scanning electron microscope (FEI Quanta 250, USA) and three dimensional microscope (VHX2000, USA) were used to observe the surface morphology of samples and its corrosion products.

### 3. RESULTS AND DISCUSSION

#### 3.1 Changes in CD during the degradation procedure of coating

Fig. 1 shows the M-S curves of the coating immersed in 5% NaCl solution for different times. The curve of the original sample (0 h) was a straight line parallel to the horizontal axis. This result indicated that the coating layer was insulated and few carriers could be migrated at this moment. After immersion for 6 h, some changes were observed in the capacitance of the coating system, which indicated that some charges were introduced into the coating with the penetration of the solution [21]. Correspondingly, the conductivity of the system was enhanced and a MIC structure was formed. Based on the M-S curves for different immersion times, the capacitance showed a gradually increasing with the immersion time prolonged. Besides, the slope of M-S curve transited from positive to negative at around  $-0.6 \text{ V}_{\text{SCE}}$  when the applied potential was scanned from  $-0.9 \text{ V}_{\text{SCE}}$  to  $-0.1 \text{ V}_{\text{SCE}}$ , indicating the predominant charger type was changed from the electron donor to the acceptor. The reason will be detailed in the discussion section. Meanwhile, the slope of the M-S curves gradually decreased during 16 day immersion, except the distinct increase observed at day 4, as shown in Fig. 1(b). This finding indicated that the CD generally increased as the immersion time prolonged, except at day 4. This condition was unfavorable for the barrier properties of the coating. Finally, the M-S curve had a positive slope at day 16, which implied that electron conduction played a dominant role at this moment.

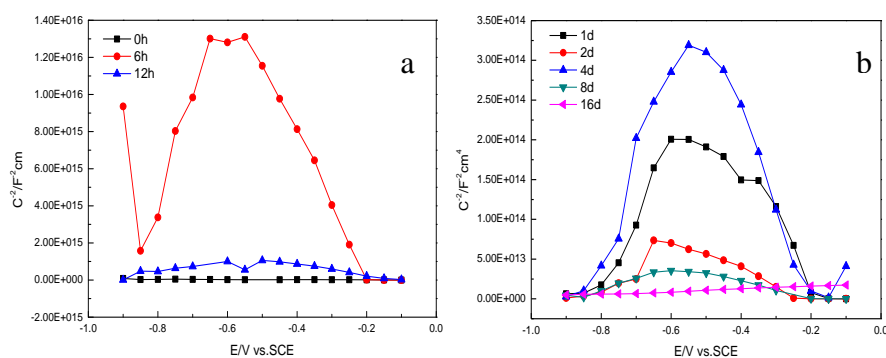


**Figure 1.** M-S plots of acrylic polyurethane coated-galvanized steel immersed in 3.5% NaCl solution: (a) immersion for 0–12 h and (b) immersion for 1–16 days.

Because the change of donor (electron) density presents the corrosion development process more directly,  $N_D$  of the coating system was used as the CD of corrosion degradation of the coating. Based on formula (1),  $N_D$  was calculated for different immersion times, in which  $\epsilon$  of acrylic polyurethane coating was taken as 6.5, as shown in Table 1. It can be seen that CD increases sharply after immersion for 2 days, and CD of the coating reaches  $10^{18} \text{ cm}^{-3}$  after immersion for 16 days, which is still much lower than that of metal ( $10^{22} \text{ cm}^{-3}$ ).

**Table 1.** CD of galvanized substrate/polyurethane coating system in 3.5% NaCl solution.

<i>Immersion time (h, day)</i>	<i>N<sub>D</sub>(cm<sup>-3</sup>)</i>
6 h	3.700E14
12 h	6.686E14
1 day	3.122E15
2 days	8.670E16
4 days	2.102E16
8 days	1.554E17
16 days	1.33E18

### 3.2 Changes in low frequency impedance during the degradation procedure of coating

According to Bierwagan, the low-frequency (LF) impedance (i.e.  $|Z|_{0.01\text{mHz}}$ ) can characterize the water penetration in a coating system, which was used to characterize the degradation of the coating system in this paper [22]. Fig. 2 shows the bode diagrams of the coated specimens. For the first two-day immersion,  $|Z|_{0.01\text{mHz}}$  decreased as the immersion time prolonged. After immersion for 4 days,  $|Z|_{0.01\text{mHz}}$  fluctuated up and down slightly.

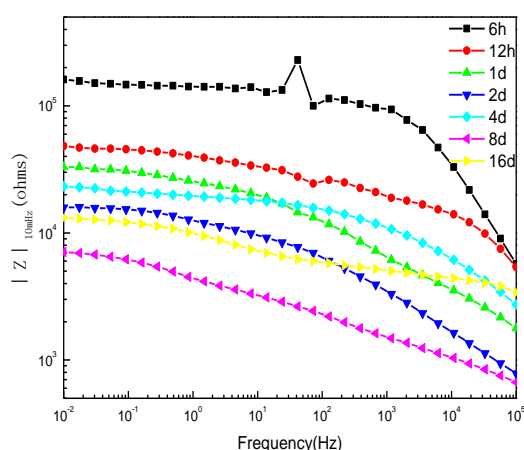


**Figure 2.** Bode diagrams of acrylic polyurethane coated galvanized steel immersed in 3.5% NaCl solution at different immersion times.

Based on the literature,  $|Z|_{0.01\text{mHz}}$  presented the protection behaviors of coating system. That is to say, the soaking process of the coating and the products generation at the interface between coating and metal substrate could be manifested with  $|Z|_{0.01\text{mHz}}$ . In this paper, the electrolyte solution kept on penetrating into the coating system through the defects of coating, resulting in the decreasing of

$|Z|_{0.01\text{mHz}}$ . The penetrating process could be divided into two stages according to the change observed in Fig. 2. The electrolyte diffused in the coating only at the first 2 days, which was manifested as one time constant. After immersion for 2 days, two time constants appeared, which indicated that the electrolyte penetrated into the interface. At this stage, electrochemical corrosion started and corrosion products were generated. Therefore, the sudden increase in the LF impedance at day 4 might be attributed to the generation of corrosion products and the blocking effect on the corrosion process, which will be discussed later.

### 3.3 Analysis of corrosion products

X-ray diffraction (XRD) measurement was performed to detect the possible corrosion product generated at the coating–substrate interface after immersion for 4 days. In this case, the varnish coating of the sample was peeled off. Thus, the corrosion products could be exposed to the detector. Fig. 3 shows the obtained spectrum.

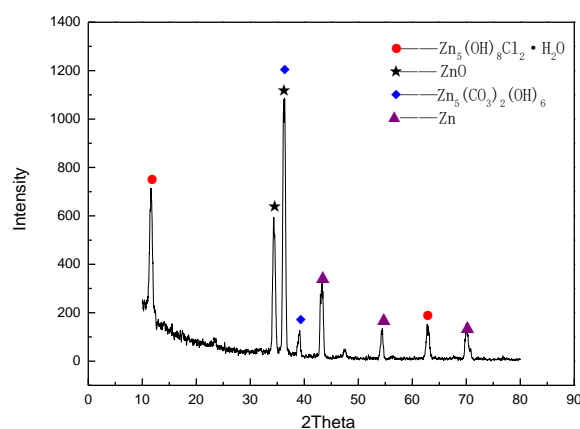


**Figure 3.** XRD spectrum of a galvanized substrate after immersion for 4 days in 3.5% NaCl solution.

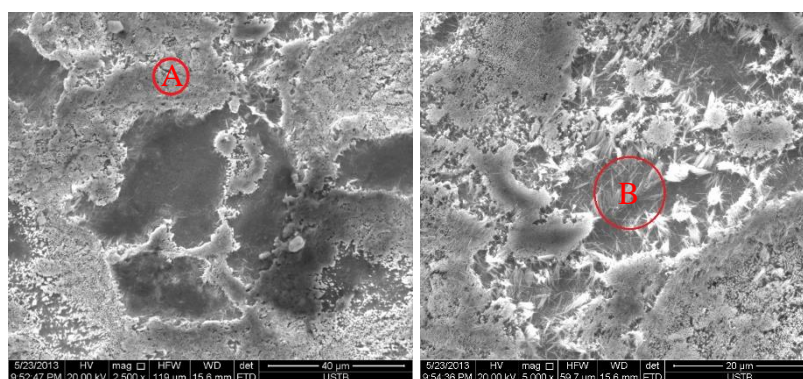


**Figure 4.** SEM micrographs of a galvanized substrate after immersion for 4 days in 3.5% NaCl solution: (a) 2500 $\times$  and (b) 5000 $\times$ .

The main products were  $Zn_5(OH)_8Cl_2 \cdot H_2O$ ,  $ZnO$ , and  $Zn_5(CO_3)_2(OH)_6$ . The corresponding corrosion morphology was observed by scanning electron microscopy, as shown in Fig. 4, in which the compact product in A area was assigned to  $Zn_5(CO_3)_2(OH)_6$ , and the needle crystals in B area could be attributed to the basic zinc chloride ( $Zn_5(OH)_8Cl_2 \cdot H_2O$ ), showing a good agreement with the results of other authors [23-25].

### 3.4 Discussion

As illustrated in literatures [15-17], the organic coating could be seen as a dielectric, which would be polarized when an electric field (EF) was applied, especially after the penetration of electrolytes into the coating. Under the present condition, the electrolyte and the metal substrate could be served as a parallel plate capacitor. Therefore, when the corrosion proceeds, the capacitance of the capacitor will be changed and subsequently affect the inner EF induced by the dipole polarization behaviors of the coating, as illustrated in Fig. 5. Due to the dependence of capacitance on the applied potential of a capacitor, the M-S method can be introduced to this work for evaluating the corrosion process of the coating. Besides,  $|Z|_{0.01Hz}$  was successfully used by Shi to monitor coating aging process [26]. Murry suggested that this parameter can characterize the entire process of coating degradation [27]. Therefore,  $|Z|_{0.01Hz}$  and CD ( $N_D$ ) were both used in this paper to assess the degradation of the coating system, as the complementary to each other.

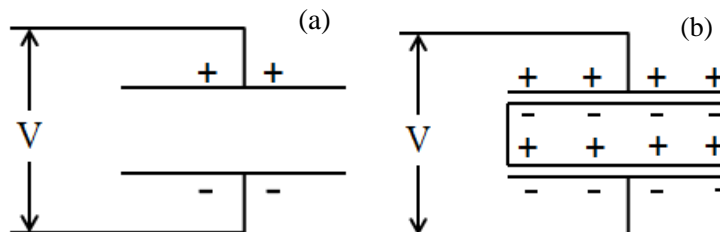


**Figure 5.** Capacitance change diagrammatic sketch of parallel plate capacitor before and after dielectric (coating) applied [16]: (a) empty; (b) dielectric applied.

#### 3.4.1 Relationship between CD and $|Z|_{0.01Hz}$ during corrosion process

As the above mentioned, the change principles of both parameters depicted the corrosion development of the coating system. Based on Fig. 6, the change of CD was negatively correlated to that of  $|Z|_{0.01Hz}$ . That is to say, the CD increased when the corrosion resistance of the coating system was deteriorated. It indicated that the diffusion or soaking process of the coating system enhanced the migration of ions and further induced the electrochemical reactions at the interface of coating and substrate, which increased the amount of donor in the dielectric (i.e. the polyurethane organic coating). With the immersion time prolonged, more and more donors were activated and started moving. Therefore, the increase in CD implied an increase in conductivity and rapid degradation of the coating [21].

It should be noted that the changing tendency of  $|Z|_{0.01\text{Hz}}$  and  $N_D$  shifted at day 4 in the current study. That is, after immersion for 4 days,  $N_D$  decreased, whereas  $|Z|_{0.01\text{Hz}}$  increased. This condition indicated that the corrosion rate slowed down. This finding might be attributed to that the corrosion products generated at the metal–substrate interface could easily fill the coating defects when the defects were small. As a result, the corrosion process was hindered. However, as the corrosion proceeded and the defects was aggravated, the protection of the coating continued to deteriorate.

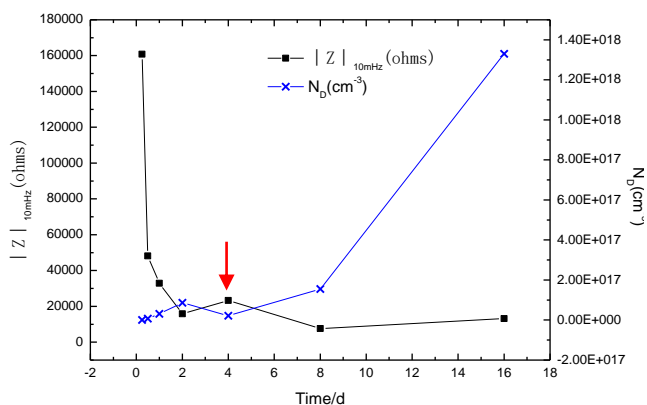


**Figure 6.** Changing curve of the CD and the LF impedance.

As a proof, corrosion products, including  $\text{Zn}_5(\text{CO}_3)_2(\text{OH})_6$  and  $\text{Zn}_5(\text{OH})_8\text{Cl}_2 \cdot \text{H}_2\text{O}$ , were found at the metal–substrate interface.  $\text{Zn}_5(\text{CO}_3)_2(\text{OH})_6$  is dense and has low solubility [28]. Studies have shown that the improvement in the corrosion resistance of the Zn–Al–Mg alloy coating is due to the formation of  $\text{Zn}_5(\text{OH})_8\text{Cl}_2 \cdot \text{H}_2\text{O}$  [29,30]. Therefore,  $\text{Zn}_5(\text{CO}_3)_2(\text{OH})_6$  and  $\text{Zn}_5(\text{OH})_8\text{Cl}_2 \cdot \text{H}_2\text{O}$  prevented the coating from penetration in the current study.

The morphology of the sample after immersion for 8 days (Fig.7) showed bubbling, rust spots, and holes on the coating surface. The shielding and insulating effects were weakened in the local area of the coating because of the generation of holes. This condition led to the decrease in corrosion resistance and the increase in electrical conductivity. As a proof, the corresponding shift could be observed in Fig. 6. As the corrosion process accelerated, the corrosion products were accumulated, which had an inhibiting effect on the penetration of the electrolyte solution. This condition prevented the diffusion of reactive ions and protected the matrix. As a result,  $|Z|_{0.01\text{Hz}}$  continuously increased at day 16. However, the coating system would present a conductive behavior and the transport of chargers would no longer be hindered once the pathway of electrolyte penetration formed in the coating system. Consequently, the conductivity was greatly enhanced, which was proven by the rapid increase in  $N_D$  after immersion for 8 days.

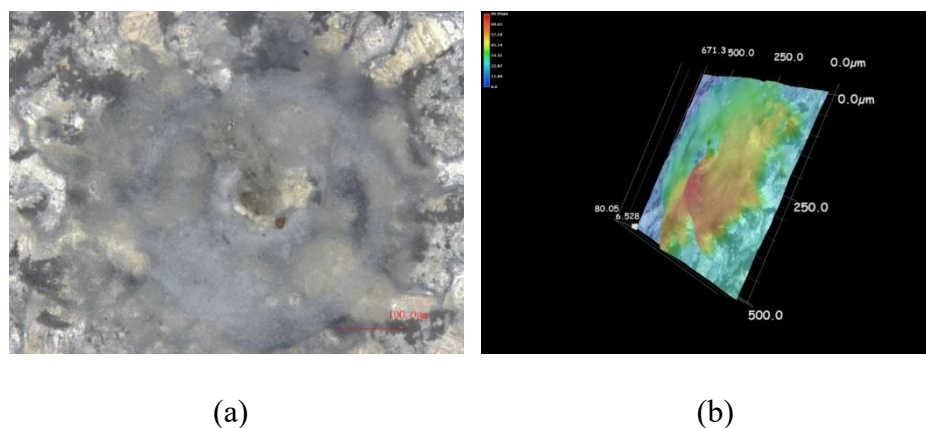


**Figure 7.** Microscopy images of acrylic polyurethane-coated galvanized steel after immersion for 8 days in 3.5% NaCl solution: (a) 2D and (b) 3D.

### 3.4.2 Effects of polarizations on the coating system

There was a transition at  $-0.6 V_{SCE}$  in the M-S curve, the slope of which changed from positive to negative, indicating that with the applied potential lifted positively, the tendency of decreasing in capacitance shifted to the increasing tendency. For this study, the open circuit potential of the system is around  $-1.0 V_{SCE} \sim -0.9 V_{SCE}$ . Therefore, when the coating system was polarized slightly from the open circuit potential, two types of polarizations exerted in the system. On one hand, when the applied external potential (absolute value) decreased, the capacitance of the parallel capacitor and that of coating induced by dipole polarization must decline consequently. But the declining rate of the capacitance for the coating should be slower than that of the capacitor due to the dipolar relaxation. On the other hand, the substrate was electrochemically polarized, which generated more and more positive chargers with the overpotential increased, i.e. zinc ions. When these two effects combined together, the changing tendency would be dependent on the predominant effect. That is to say, when the overpotential was not big enough, the polarization of capacitor was dominant, resulting in the decrease of the total capacitance. On the contrary, the electrochemical polarization became the controlling effect when the overpotential was higher than  $-0.6 V_{SCE}$ . However, the effect of electrochemical polarization would be weakened, because the formation of corrosion product, such as ZnO, made the substrate more stable after immersion for 16 days. Therefore, the capacitance presented a continuous drop for the 8-day curve in Fig. 1, with the decrease of applied external potential (absolute value).

In addition, the penetration of electrolyte into the coating intensified the dipole polarization of the coating because more dipoles were activated. To keep EF intensity unchanged, more chargers must migrate to the plate of the capacitor, resulting in an increase of capacitance. This could be used to explain why the capacitance (C) rose with the prolonged immersion time for one specific applied potential (E) in Fig.1.

## 4. CONCLUSIONS

Based on the above results, the following conclusions can be drawn:

- (1) In general, the process of the corrosion development could be manifested as the increase in

the CD and the decrease in  $|Z|_{0.01\text{Hz}}$  until the coating system was destroyed.

(2) The generation of corrosion products  $\text{Zn}_5(\text{OH})_8\text{Cl}_2 \cdot \text{H}_2\text{O}$  and  $\text{Zn}_5(\text{CO}_3)_2(\text{OH})_6$ , which could improve the corrosion resistance of substrate, led to the decrease of CD. But after a penetrating hole was established between the coating and the substrate in the coating, it was hard to evaluate the following corrosion process with CD.

(3) Two types of polarizations, dipole polarization and electrochemical polarization, exerted their efforts in the coating system during corrosion degradation process. The one playing the dominant role was dependent on the corrosion process.

#### ACKNOWLEDGEMENTS

The authors gratefully acknowledge the financial support provided by the National Natural Science Foundation of China (U1560104), and the National Materials Corrosion and Protection Data Center.

#### References

1. J. M. McIntyre and H. Q. Pham, *Prog. Org. Coat.*, 27 (1996) 201.
2. P. L. Bonora, F. Deflorian and L. Fedrizzi, *Electrochim. Acta*, 41 (1996) 1073.
3. J.B. Jorcin, E. Aragon and C. Merlatti, *Corros. Sci.*, 48 (2006) 1779.
4. M. Doherty and J. M. Sykes, *Corros. Sci.*, 46 (2004) 1265.
5. Luo Bing, A. T. Xu and Y. S. Liang, *Int. J. Electrochem. Sci.*, 7 (2012) 8859.
6. J. Q. Zhang and C. N. Cao, *Corros. & Prot.*, 19 (1998) 99.
7. T. Hamada and H. Nomura, *Prog. Org. Coat.*, 37 (1999) 141.
8. J. M. Sykes, E. P. Whyte and X. Yu, *Prog. Org. Coat.*, 102 (2017) 82.
9. F. Y. Lu, B. D. Song, and P. He, *RSC Adv.*, 7 (2017) 13742.
10. M. A. Hernández, N. Masó and A. R. West, *Appl. Phys. Lett.*, 108 (2016) 152901.
11. K. Darowicki and L. Gawel, *Electrocatalysis*, 8 (2017) 235.
12. Z. H. Chen, C. He and F. Yu, *Int. J. Electrochem. Sci.*, 12 (2017) 2798.
13. B. R. Hinderliter, S. G. Croll and D. E. Tallman, *Electrochim. Acta*, 51 (2006) 4505.
14. Q. D. Zhong, J. Zheng and N. X. Xu, *Corros. Sci. and Prot. Tech.*, 16 (2004) 276.
15. Q. D. Zhong, R. Michael, Z. Zhang and J. Zheng, *J. Electrochem. Soc.*, 151 (2004) 7.
16. C. Wang, M. Q. Sheng, Q. D. Zhong, *Acta Chim. Sinica*, 67 (2009) 709.
17. C. Wang, Q. D. Zhong, K. C. Chou, X. G. Lu, *Acta Phys-Chim. Sin.*, 24 (2008) 1277.
18. S. R. Morison, 'Electrochemistry at Semiconductor and Oxidized Metal Electrodes', (1980) Plenum Press, New York.
19. J. Sikors, E. Sikora and D. Macdonald, *Electrochim. Acta*, 45 (2000) 1875.
20. P. Schmuki and H. Bohni, *Electrochim. Acta*, 40 (1995) 775.
21. Y. Xiao and J. f. Gu, *Arab. J. Sci. Eng.*, 42 (2017) 4273.
22. G. Bierwagen, D. Tallman, J. P. Li, L. Y. He and C. Jeffcoate, *Prog. Org. Coat.*, 64 (2009) 466.
23. P. R. Sere, M. Zapponi and C. I. Elsner, *Corros. Sci.*, 40 (1998) 1711.
24. S. Schürz, G. H. Luckeneder and M. Fleischanderl, *Corros. Sci.*, 52 (2010) 3271.
25. K. Zhang and R. B. Song, *Int. J. Electrochem. Sci.*, 14 (2019) 1488.
26. A. K. Singh, S. Alam and N. Rani, *Trans. Inst. Met. Finish.*, 95 (2017) 165.
27. J. J. Santana and J.E. González, *Int. J. Electrochem. Sci.*, 7 (2012) 6489.
28. X. G. Zhang. (1996) Electrochemistry of Zinc Oxide. In: Corrosion and Electrochemistry of Zinc. Springer, Boston, MA
29. S. Tanaka, K. Honda, A. Takahashi, Y. Morimoto, M. Kurosaki, H. Shindo, K. Nishimura and M.

Sugiyama, Proc. 1st Int. Conf. on 'Zinc and Zinc Alloy Coated Steel', Brussels, Belgium, June (2001) 153.

30. K. Nishimura, H. Shindo, K. Kato and Y. Morimoto, Proc. Galvatech'98, Int. Conf. on 'Zinc and Zinc Alloy Coated Steel', Chiba, Japan, September (1998) 437.

© 2019 The Authors. Published by ESG ([www.electrochemsci.org](http://www.electrochemsci.org)). This article is an open access article distributed under the terms and conditions of the Creative Commons Attribution license (<http://creativecommons.org/licenses/by/4.0/>).